communications earth & environment

ARTICLE

https://doi.org/10.1038/s43247-023-00801-w OPEN

Biophysical flocculation reduces variability of cohesive sediment settling velocity

L. Ye[1,2,3✉], J. A. Penaloza-Giraldo[3], A. J. Manning[3,4,5], J. Holyoke[3,6] & T.-J. Hsu[3]

Biophysical cohesion, introduced predominantly by Extracellular Polymeric Substances (EPS) during mineral flocculation in subaqueous environments, plays important role in morpho-dynamics, biogeochemical cycles and ecosystem processes. However, the mechanism of how EPS functioning with cohesive particles and affects settling behaviors remain poorly understood. We measure initial flocculation rate, floc size and settling velocity of mineral and artificial EPS (Xanthan gum) mixtures. Combining results from these and previous studies demonstrate coherent intensification of EPS-related flocculation compare with those of pure mineral and oil-mineral mixtures. Importantly, the presence of EPS fundamentally changes floc structure and reduces variability of settling velocity. Measured data shows that ratios of microfloc and macrofloc settling velocity for pure mineral flocs is 3.9 but greatly reduced to a lowest value of 1.6 due to biological EPS addition. The low variability of settling velocity due to EPS participation explains the seemingly inconsistent results previously observed between field and laboratory studies.

[1] School of Marine Sciences, Sun Yat-sen University, Zhuhai, China. [2] Southern Marine Science and Engineering Guangdong Laboratory (Zhuhai), Zhuhai, China. [3] Department of Civil and Environmental Engineering, Center for Applied Coastal Research, University of Delaware, Newark, DE, USA. [4] HR Wallingford Ltd., Coasts and Oceans Group, Wallingford, CT, USA. [5] School of Biological and Marine Sciences, University of Plymouth, Plymouth, UK. [6] Department of Civil, Architectural and Environmental Engineering, University of Texas at Austin, Austin, TX, USA. ✉email: yeleiping@mail.sysu.edu.cn

Mud in subaqueous environment generally consists of organic materials (e.g., extracellular polymeric substances (EPS)[1]) and inorganic mineral clays[2]. They are transported as flocs with a wide variety of physical properties, such as settling velocity and porosity/density that are of interest in understanding coastal and estuarine morphodynamics[3,4], biogeochemical nutrient cycling[5,6], carbon and pollutant transport[7,8], and ecosystem functions[9]. A good understanding of flocculation dynamics is also crucial to predict the impact of erosion and sedimentation when being confronted with sea level change, land-use shortage, waterway navigability, and scour around engineering infrastructure[10,11].

Particle settling velocity is one of the most important quantity in the study of sediment transport[12–14]. Due to flocculation, estimating settling velocity of cohesive sediment is difficult and it is usually measured by video cameras or laser diffraction devices[15–17]. Most laboratory studies focus on inorganic clay/silt particles that show large variability of measured settling velocity as function of floc size and mineral types[18–20]. On the contrary, many field observations in coastal environments have reported that a floc settling velocity of around $1\,mm{\cdot}s^{-1}$ is a robust estimate[21,22] implying a rather low variability of floc settling velocity[23,24]. In fluvial environment, Lamb et al.[25] report that clay minerals and silt particles may settle as flocs with a nearly uniform settling velocity of $0.34\,mm{\cdot}s^{-1}$. They further conjecture that the reason why floc can form in freshwater is possibly due to high organic content via sticky EPS.

Microbial EPS has been considered one of the natural flocculants[26], however, its effect on settling velocity of floc are not fully understood[27]. EPS is products of biochemical secretions and can make up as much as 50~90 % of the organic matter content of microbial aggregates[28,29]. EPS has distinctive characteristics in composition and densities that are different from the minerals or other organic particles in suspension[30]. However, being anionic polyelectrolytes, EPS have somewhat similar flocculation mechanism with synthetic anionic flocculants such as polyacrylamide. It has been reported to cause bioflocculation via the divalent cation bridging (DCB) mechanism, whereby divalent cations such as Ca^{2+} and Mg^{2+} form bridges between anionic groups of EPS and negatively charged particles[31] and reduce the electrostatic repulsion between the particles due to the compressed double layer. Similar mechanism of DCB has also been reported for anionic polyacrylamide flocculation of mineral (kaolinite) particles[32,33].

In natural water environments, flocculation dynamics involve complicated mixtures of multiple types of cohesive particles[34]. Most clay minerals and EPS possess charges or functional groups that promotes floc formations[35]. It is well-established that floc formation is controlled by the intermolecular and surface forces between clay particles and EPS molecules, including van der Waals attractions[36], Coulomb forces[37], hydrogen bond[38], and ion-dipole forces[39], among others. These clay-EPS interactions are further complicated by water chemistry, clay surface's electrical double layers, and associated clay-clay interactions[40–42]. The EPSs act as polymeric bridges between particles to build large, settlable flocs[43], which may otherwise be kept apart by the double layer repulsion[44,45]. Therefore, the geometrical conformation and length of EPS molecules also affect clay-EPS interactions. The multivalent cations can further enhance the formation of polymeric bridges by connecting between the functional sites of EPSs and the negatively charged sites of mineral particles[46]. The EPSs and binding cations mitigate the overall negative surface charge of particles, thereby increasing the flocculation potential of particles[47–49]. A group of such clay particles bridged by EPS molecules make up a loosely associated floc. As a result, the size of clay-EPS flocs depends on these interactions as well as the physical and chemical properties, mainly 'stickiness', of the two types of constituents, clay minerals, and EPSs. Clearly, EPSs play an important role in flocculation and are a key component in the heterogeneous composition of flocs.

In marine environments, EPS has been observed to form large-sized flocs (>5 mm), or called "marine snows", on the sea up to several meters in size[50], which aggregate with other particles in suspension such as minerals and pollutant-like spilt oil[51,52]. The physical interparticlle bonds provided by EPS are observed to increase the tensile strength of the mud fraction[53] and enhance mixed biophysical cohesion[54]. Therefore, quantification of the stickiness between specific types of cohesive particles becomes crucial for determining floc properties (size, density, and settling velocity) and flocculation dynamics[55,56]. Previous studies generally utilize an empirical cohesion coefficient to represent the stickiness value of particles[57,58]. However, multiple particles mixtures may behave very differently in aggregate characteristics during flocculation process. Most importantly, the main characteristic of EPS is to enhance aggregation of suspended cohesive particles dramatically[59] although the natural EPS may show much complexity in various fractions such as protein and polysaccharide due to microorganism species. Exsiting studies on the quantification of cohesion and the resulting floc properties due to the participation EPS is rare. The research gap regarding how the participation of EPS in the formation of flocs of cohesive sediment can modify the floc size, density, and the resuting settling velocity need to be further addressed.

The objective of this study is to quantify the effect of EPS on the variability of floc settling velocity. We provide quantitative evidence that bio-cohesion greatly enhances the stickiness during flocculation, which dominates over the London-van der Waals force and electrostatic bonding forces and hence the effect of clay type and salinity becomes unimportant. As a result, bio-cohesion drastically reduces the variability of floc settling velocity as a function of floc size and clay type. Our findings explain the field observed low variability of floc settling in fluvial and coastal environments due to the dominance of bio-cohesion.

Results

Quantifying stickiness of minerals and EPS flocculation. Eight cases of different collective mixture of minerals and EPS (C01 to C06 in saltwater with salinity 35 psu and C07 to C08 in freshwater condition, Table 1) show distinctly different flocculation rates during the first 3~5 minutes of floc generation. Here, the initial flocculation rate (IFR) is utilized to quantify the stickiness of each case, which is proportional to the magnitude of IFR. For the saltwater cases without EPS addition (C01 to C03), mineral particles themselves show a wide range of IFR or stickiness (Fig. 1a, b). The lowest stickiness is Kaolinite (C01) with IFR =

Table 1 A summary of samples used in each case of the jar experiment.

Cases/Samples		Kaolinite clay (K)	Bentonite clay (B)	Xanthan gum (EPS)	Salinity
		mg	mg	mg	‰
C01	K	500	/	/	35
C02	B	/	500	/	35
C03	K + B	250	250	/	35
C04	K + EPS	500	/	500	35
C05	B + EPS	/	500	500	35
C06	K + B + EPS	250	250	500	35
C07	K + EPS	500	/	500	0
C08	B + EPS	/	500	500	0

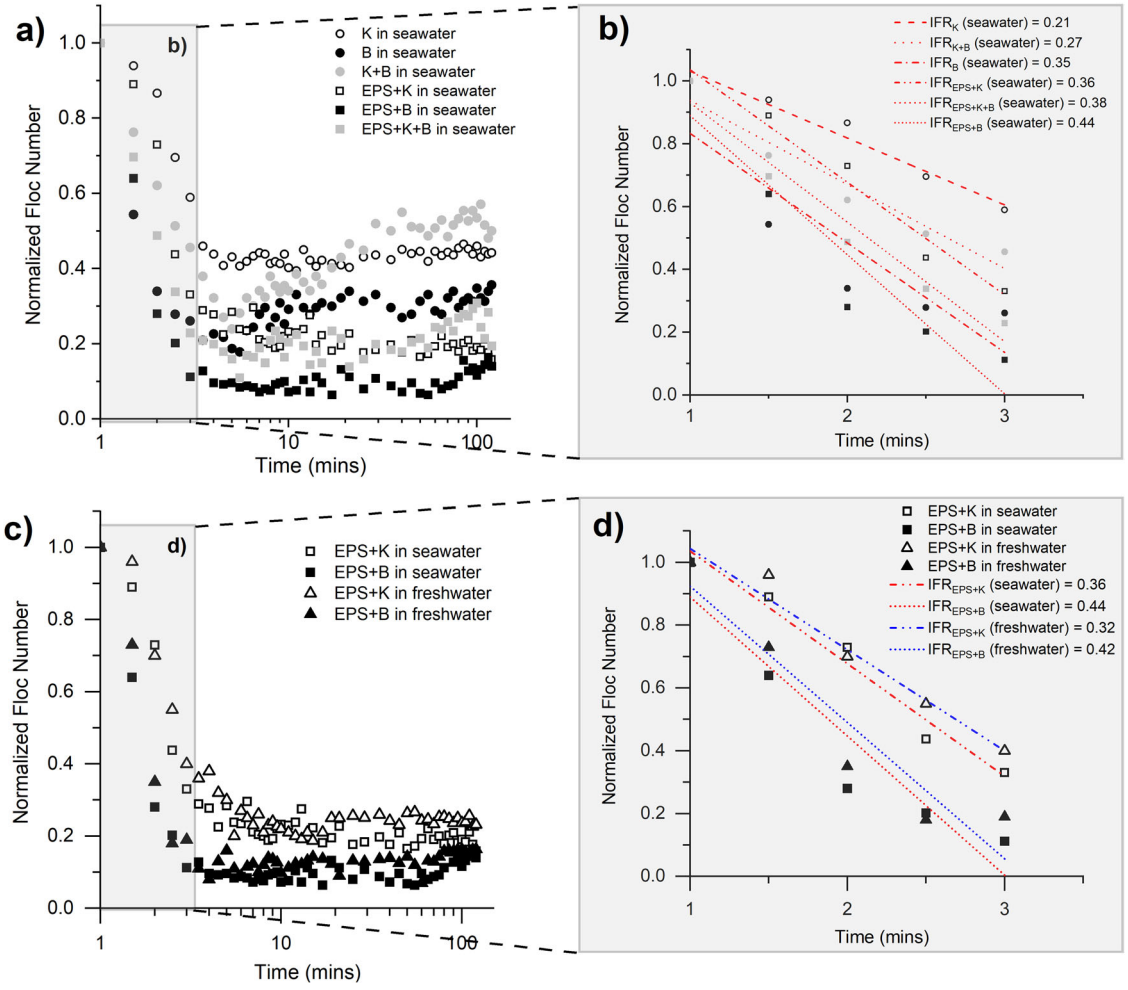

Fig. 1 Temporal evolutions of normalized floc numbers in each studies case. a, **b** are temporal evolutions of normalized floc numbers for six saltwater cases: Kaolinite (K, blank circles, C-01), Bentonite (B, solid circles, C-02), 1:1 mixed Kaolinite and Bentonite (K + B, gray circles, C-03), EPS-Kaolinite (EPS + K, blank squares, C-04), EPS-Bentonite (EPS + B, solid squares, C-05), EPS-Kaolinite-Bentonite (EPS + K + B, gray squares, C-06); **c**, **d** show that the temporal evolutions of two freshwater samples for EPS-Kaolinite (C-07) and EPS-Bentonite (C-08) are similar to their saltwater counterparts. The initial particle number of each case measured from high-resolution image was used for number normalization. The shadowed area **b** and **d** represents the zoom-in of the initial 3 minutes emphasizes the initial floc numbers changes, and the slopes quantify the initial flocculation rates.

0.21 while the highest is Bentonite (C02) with IFR = 0.35 (Fig. 1b). Therefore, these two mineral types cause a factor 0.35/0.21 = 1.67 change in stickiness in seawater.

Adding EPS to mineral flocs clearly increases the resulting floc stickiness in seawater (Fig. 1b). For instance, looking into the IRF of Kaolinite cases (C01 and C04), including EPS increases stickiness of Kaolinite floc by more than 70 % in seawater. For Bentonite floc (compare C02 and C05), the stickiness increases by only 26 %. As a result, adding EPS reduces the resulting the variability of particles stickiness due to mineral type. Considering the higher stickiness in EPS-Bentonite mixture (IFR = 0.44) and the lower stickiness in EPS- Kaolinite mixture (IFR = 0.36), a considerably lower variability of factor 0.44/0.36 = 1.22 is obtained (compare to 1.67 for a much larger variability without EPS participation). Essentially, the EPS effect on increasing stickiness for Kaolinite particles is nearly three times greater than that for Bentonite. As Bentonite particles behave much stickier in seawater than Kaolinite, adding EPS only slightly increases its stickiness. On the contrary, for the less cohesive Kaolinite particles, EPS plays a dominating role in determining the overall stickiness.

In freshwater condition, the addition of EPS to Kaolinite and Bentonite show similar IFRs to those in seawater (Fig. 1c, d). For Kaolinite and EPS flocculation in freshwater (C07), the IFR reduces only slightly by around 10 % compared to saltwater, while for Bentonite and EPS (C08), the IFR reduction is only 5 %. The flocculation functions by EPS is clearly dominant in subaqueous environments. Ye et al.[60] reported that the physical properties of flocs can be quite different for specific mineral types when the cohesion of mineral particles controls floc aggregation and breakups. With the presence of EPS dominating the cohesion during flocculation, the corresponding floc characteristics may be importantly modified.

How dose EPS change floc structures? High-resolution microscopy images show unique structures of different mineral and EPS-mineral flocs. These distinct floc structures are resulted from each type of mineral particles' properties and bio-cohesion and they may be directly associated with stickiness. The pure Kaolinite particles having the lowest stickiness tend to form much smaller-sized flocs with a more compact structure (Fig. 2a) than those of Bentonite flocs (Fig. 2b). Examining a small number of larger Kaolinite floc, it is evident that they are of much lower porosity (Fig. 2a) than the Bentonite flocs where the higher transparency porous structure can be seen (Fig. 2b). The 1:1

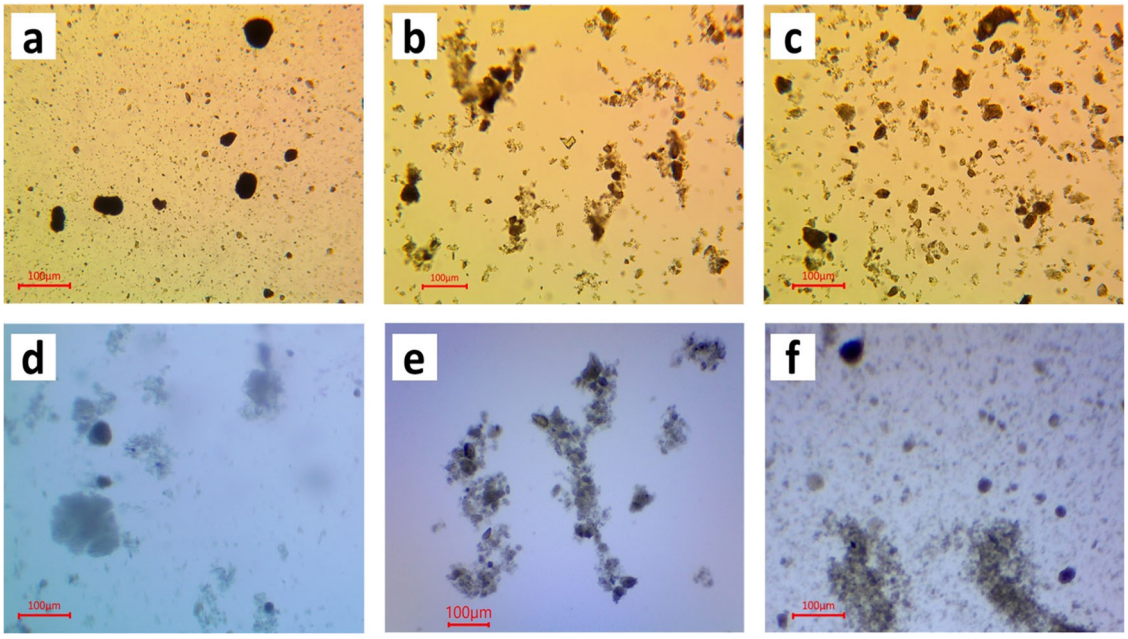

Fig. 2 Floc images obtained from the high-resolution microscopy analysis. a Kaolinite floc (C-01); **b** Bentonite floc (C-02); **c** mixed Kaolinite and Bentonite floc (C-03); **d** mixed EPS and Kaolinite floc (C-04); **e** mixed EPS and Bentonite floc (C-05); **f** mixed EPS, Kaolinite and Bentonite floc (C-06).

mixed Kaolinite and Bentonite flocs appear to consist of both types of floc structures (Fig. 2c).

With the addition of equivalent amount of EPS, all three mineral cases show the formation of considerably larger and porous flocs (Fig. 2d–f). Although Kaolinite and Bentonite clay show evident differences in mineral particles' stickiness and thereby floc structures (Fig. 2a, b), the same amount of EPS addition enlarges floc size and porosity in both clay types (Fig. 2d, e). Particularly for Kaolinite floc, a large number of small flocs disappear after the addition of EPS and the resulting large-sized floc are dominated by the higher porosity EPS-web structure (Fig. 2a, d). Meanwhile, the shape and structure of the EPS-Bentonite flocs appear to be qualitatively similar to those of pure Bentonite, except that the floc number (floc size) is dramatically reduced (increased) (Fig. 2b, e). For the 1:1 mixture of Kaolinite and Bentonite, adding EPS tends to bond together many smaller mineral flocs to form large porous floc bodies (Fig. 2c, f). These floc images reveal the role of sticky EPS in homogenize the aggregate structure of different clays, and this distinct effect is expected to modify the physical properties of floc to be quantified in the next section.

How does EPS change floc density, settling velocity, and fractal dimension? The results analyzed by the 2nd version of Laboratory Spectral Flocculation Characteristics instrument (LabS-FLOC-2 system, see the Methods section) for floc numbers (Fig. 3a, c), effective density (Fig. 3d, f), settling velocity (Fig. 3g–i) and fractal dimension (Fig. 3j–l) in 12 size bands (Fig. 3m) reveal the vital role of EPS in controlling physical properties of flocs. EPS addition clearly increases the floc numbers in large-size bands (SB) of Kaolinite (SB6-8) and Bentonite (SB8-12) (Fig. 3a, b). Since the total floc mass must conserve, increased floc number in larger SB causes a reduction of floc number in smaller SB. Specifically, adding EPS reduces the floc number in size bands smaller than 160 μm in Kaolinite (Fig. 3a) and 80 μm in Bentonite (Fig. 3b). This is consistent with the image shown in Fig.2d, e that EPS produces large flocs by connecting smaller flocs via its mucus web structure. A similar but less pronounced trend is observed by adding EPS to the Kaolinite and Bentonite mixture (Fig. 3c).

Since EPS has a very lower effective density (~33~200 $kg{\cdot}m^{-3}$)[61] than the mineral effective density (~1650 $kg{\cdot}m^{-3}$), the presence of EPS can importantly reduce the effective density of large Kaolinite flocs (floc size >160 μm) (Fig. 3d), and their settling velocity is also reduced by a factor 2~3 (Fig. 3g). Specifically, for flocs larger than 160 μm, pure Kaolinite has a settling velocity ranging from 4~8 $mm{\cdot}s^{-1}$, while the EPS and Kaolinite mixture shows a much narrower range of 3~4 $mm{\cdot}s^{-1}$ (Fig. 3g). Adding EPS also reduces the density of large Bentonite flocs (floc size >320 μm) while contrarily, slightly increases the density of smaller Bentonite flocs (floc size <320 μm) (Fig. 3e). This results in an even lower settling velocity variability as a function of floc size (Fig. 3h). For floc size greater than 120 μm, pure Bentonite settling velocity ranges from 1.5~6 $mm{\cdot}s^{-1}$, but Bentonite and EPS mixture shows a much narrower range of 2.5~4 $mm{\cdot}s^{-1}$ (Fig. 3h). Adding EPS to Kaolinite and Bentonite mixture reduces floc density throughout the entire floc spectrum with a more important reduction for floc size larger than 320 μm in SB8-10 (Fig. 3f). This also narrows the variability of floc settling velocity to between 0.5~2 $mm{\cdot}s^{-1}$ (Fig. 3i) for floc size greater than 120 μm while the pure Kaolinite and Bentonite mixture shows a very wide range of settling velocity between 2~11 $mm{\cdot}s^{-1}$.

Our finding that the addition of EPS importantly reduces the settling velocity variability may be a remarkable implication for natural flocs with mixed types of cohesive materials. The general recommendations that the floc settling velocity is around 1 $mm{\cdot}s^{-1}$ in estuaries[21,22,62] and is around 0.34 $mm{\cdot}s^{-1}$ in the fluvial environments[25] are very likely due to bio-cohesion. The settling process of cohesive particles in natural subaqueous systems may be much stable and predictable with the participation of pervasive biological sticky materials.

Fractal dimension is a useful parameter to quantify the porosity and shape of flocs[63]. A fractal dimension as low as 2 or smaller indicates a high floc porosity and typically a elongated shape[64]. Adding EPS to Kaolinite, the fractal dimension is reduced from 2.5 to about 2.2~2.4 (Fig. 3j). Interestingly, adding EPS to Bentonite slightly increases the fractal dimension of small-sized flocs (Fig. 3k). EPS addition results in the loose small Bentonite floc structure becoming more compact. However, for large-sized

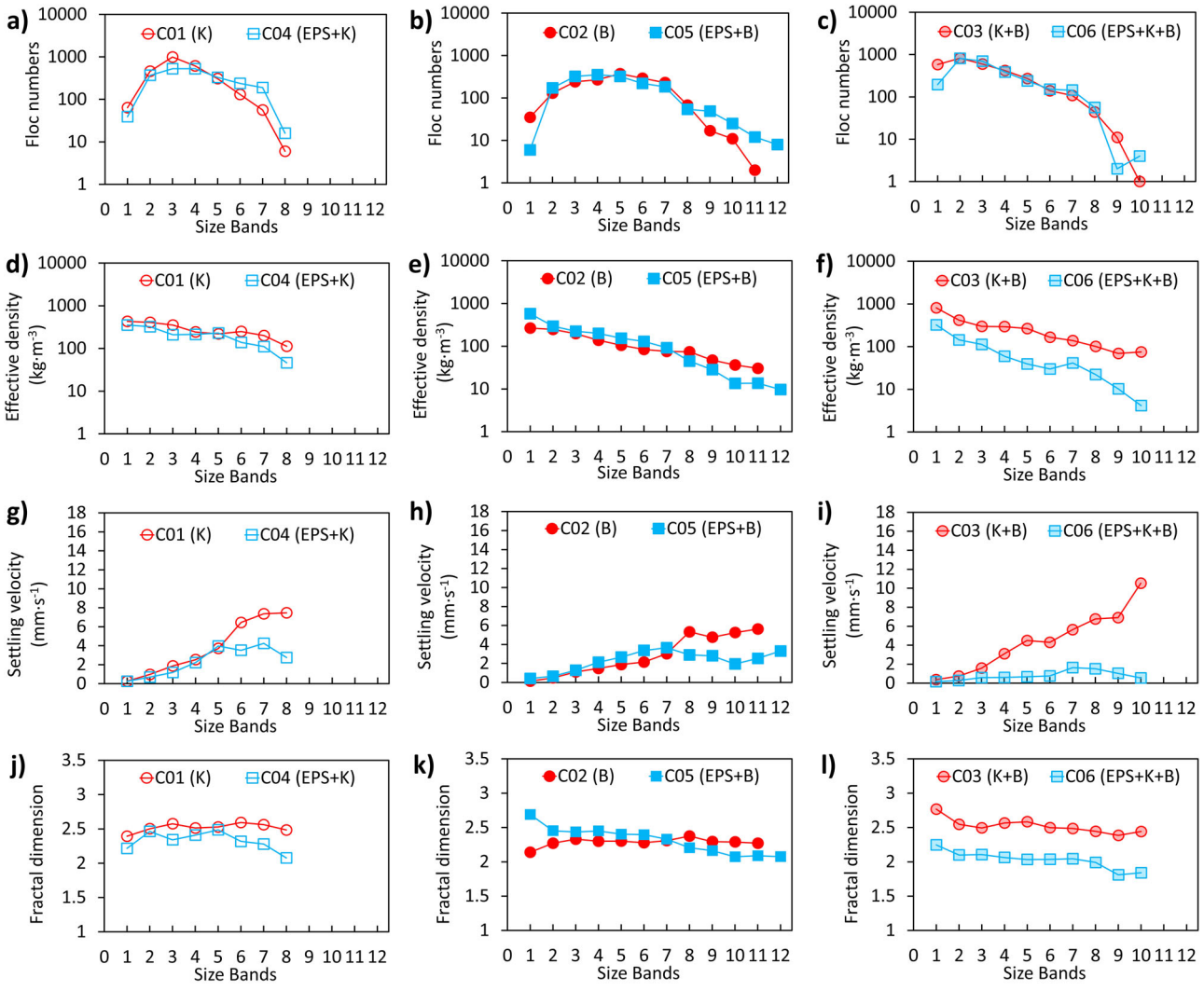

m)

Size Band	1	2	3	4	5	6	7	8	9	10	11	12
Size Range (μm)	20-40	40-80	80-120	120-160	160-200	200-240	240-320	320-400	400-480	480-560	560-640	>640

Fig. 3 Floc properties obtained from LabSFLOC-2.0 analysis of saltwater cases. a–l Show the size spectra, expressed in 12 size bands (see **m**), of floc numbers (**a**–**c**), effective densities of flocs (**d**–**f**), settling velocities of flocs (**g**–**i**), and fractal dimension (**j**–**l**) in Kaolinite-related cases (**a**, **d**, **g**, **j**), Bentonite-related cases (**b**, **e**, **h**, **k**), and mixed kaolinite and bentonite cases (**c**, **f**, **i**, **l**), respectively.

Bentonite flocs, adding EPS shows an expected reduction of fractal dimension from 2.4 to 2.2 (Fig. 3k). Introducing EPS to a Kaolinite-Bentonite mixture, the fractal dimension is importantly reduced from 2.5 to 2.0 (Fig. 3l). Again, the reduction of fractal dimensions is consistent with the EPS web and gel structures bonding with mineral flocs, which influences the porosity and shape of the flocs especially in large size bands that generally contain more EPS constituent.

Discussion and conclusions

In cohesive sediment studies, the flocs are often classified by microflocs and macroflocs with a demarcation floc size set to be 160 μm[65,66]. The mean values of the floc settling velocity for each case are summarized in Table 2. Results again reveal that the pure mineral flocs generally show dramatic differences in settling velocity between macroflocs and microflocs (a ratio of 2.7, 2.4, and 3.9 for Kaolinite, Bentonite, and Kaolinite-Bentonite mixture, respectively). When EPS participates in the flocculation process, the mucus structure provides unique capabilities with a much greater stickiness to connect mineral particles/flocs that dominates the mineral cohesion and reduces the difference of settling velocity between microflocs and macroflocs (a ratio of 2.1, 1.5, and 1.6 for Kaolinite, Bentonite, Kaolinite-Bentonite mixture, respectively). In natural subaqueous environment, flocculation process can be highly influenced by multiple environmental factors, such as salinity and bio-cohesion[67,68]. In freshwater, flocculation occurs primarily due to bio-cohesion[25] (Fig. 1c). Algae bloom has been considered as the main contribution to the formation of large-sized macroflocs[69]. After all, biological EPS fraction may vary in natural water, but with generally high EPS production in estuarine and coastal ecosystems, its role in the flocculation process can importantly affect natural cohesive flocs settling characteristics and their depositional prediction[66].

Results presented here also provide an explanation of the recent work by Ye et al.[27], who show the participation of EPS in oil-mineral aggregates (OMAs)[70,71] importantly reduces the variability of settling velocity as a function of floc size. Using IFR to quantify stickness in the pure mineral and EPS-mineral samples in saline water and freshwater, this work provides

Table 2 Summary of the mean settling velocity of microflocs (<160 μm) and macrofloc (>160 μm) fraction of each saltwater samples (C-01 to C-06) and comparable data from oil participated mineral and EPS floc samples reported by Ye et al. (2021).

Cases/Samples	Data source	Mean settling velocity (mm s^{-1})			
		all	microflocs	Macroflocs	microfloc/Macrofloc
K[a]	This study.	2.41	1.82	4.89	0.37
B[b]		2.01	1.08	2.61	0.41
K + B		1.97	1.27	4.90	0.26
EPS[c] + K		2.26	1.61	3.37	0.48
EPS + B		2.29	1.81	2.83	0.64
EPS + K + B		0.87	0.64	1.02	0.63
K + O[d]	Ye et al.[27]	1.21	1.03	2.41	0.43
B + O		2.53	1.07	3.36	0.32
K + B + O		3.33	1.94	7.63	0.25
EPS + K + O		1.16	1.11	1.36	0.82
EPS + B + O		2.89	2.03	2.76	0.74
EPS + K + B + O		1.14	0.74	2.08	0.36

[a]Kaolinite.
[b]Bentonite.
[c]EPS-Xanthan gum.
[d]Organic Pollutant (Crude oil).

quantitative evidence on the role of EPS in homogenize the variability of floc settling velocity. In coastal subaqueous environment largely influenced by human activities, cohesive mineral particles, and biological fractions tend to aggregate with particulate pollutants, as well as aqueous contaminants such as droplets of spilt oil[72,73]. Due to a much larger cohesion of Bentonite with fastest aggregation at initial flocculation phase (see Fig.1), Kaolinite and Bentonite particles respond to oil differently[60]. Oil and lower cohesion Kaolinite particles form droplet-OMAs with a reduced effective density because the oil droplets remain largely intact. On the contrary, oil and more cohesive Bentonite particles form flaky OMAs with a slightly increased density. Hence, the resulting settling velocities are highly dependent on floc size (microflocs or macroflocs) and mineral type. As shown in Table 2, the macrofloc and microfloc settling velocity of oil-Kaolinite, oil-Bentonite, oil-Kaolinite-Bentonite mixture show a factor 2, 3, and 4 difference in their settling velocities, respectively. With the addition of EPS in these three oil-mineral cases, the settling velocity between microfloc and macrofloc show much lower variability of a factor, 1.2, 1.36, and 2.8, respectively[27]. Therefore, adding EPS to OMAs also tends to erase the effect of mineral types on the variability of settling velocity.

In summary, the experimental study presented here examined the importance of combined physical and biological stickiness provided by mineral clays and extracellular polymeric substances (EPS). Measured data reveals the prevailing effect of biological stickiness on flocculation and floc settling velocity. EPS is by far the most effective in determining aggregate characteristics due to a much stronger stickiness quantified in this study by the IFR. Microscope images confirm that with the EPS participation, the aggregate structures formed by different mineral clays become very similar due to the homogenization by the web structure of the low-density mucus.

Moreover, the effect of EPS has been shown to reduce the variability of four key physical characteristics of flocs (floc size, effective density, settling velocity, and fractal dimension) importantly by up to several factors. The key finding that the EPS participation in the mineral flocculation importantly reducing the variability of settling velocity explains the general consensus that flocs settling velocity in estuaries is around 1 mm·s^{-1} even lower[22]. Some most recent studies also have shown that fine sediments in the fluvial environments settle as flocs with a surprisingly low variability of settling velocity (~0.34 mm·s^{-1})[25] and very low variability of OMA settling velocity with high organic content[27]. Changes induced by biological cohesion and its interaction with physical cohesnion render the existing flocculation and settling flux predictors for natural cohesive materials inadequate for many subaqueous environments. The present results provide a strong evidence on the effect of bio-cohesion on flocculation and settling velocity of cohesive sediments and warrent more extensive future research to improve its prediction.

Methods

Floc generation. A self-designed experimental jar-test set[60] and eight different cases are set up to generate flocs of different mineral and artificial EPS content for saline water (C01 to C06, see Table 1) of 35 PSU and freshwater (C07 to C08) at a constant turbulence levet in a 1000 ml jar. Two most common clay types with large difference in cohesion in saline water: white Kaolin clay (92.3 ± 2.5 % Kaolinite) and Wyoming sodium Bentonite clay (85.2 ± 2.3 % Montmorillonite) with initial particle concerntration of 500 mg·l^{-1}, respectively are used to generate flocs.

Initially, the corresponding mineral clay and/or Xanthan (in dry powder) are weighted according to the cases to be added to the specific jar. Xanthan gum has been successfully applied in cohesive sediment transport experiments in simulating biological sticky mucus physical function in many previous labortary studies[1,54]. Differently from the subaqueous bed substrates, for the fine suspended particles forming flocs, most components can be cohesive materials (>90 %) including mineral clays, organic matters, contaminants etc. This also explains why the floc effective density can vary in a wide range (200~1600 mg·m^{-3}) and the more EPS contained in a floc, the lower floc density is. In natural environments, the EPS % with a suspended floc mostly vary from 5 % (almost pure mineral flocs) to 95 % (marine snow)[50]. In the experimental tests, we selected a median amount of EPS (50 %) for the input cohesive mixtures which can be representative for the mixture flocculation standard. The mixture in each sample is mechanically mixed with extremely strong stirring speed (~1000 rpm) for about 2 minutes to break any floc into minimum-sized primary particles. Subsequently, the stirring speed is reduced and maintained at 490 rpm for 2 hours to reach the steady/equilibrium state as demonstrated in Ye et al.[60]. The three-component flow velocity were measured by a Vectrino Profiler (Nortek), which was mounted on the shelf above the magnetic stirrer with the sensor probes located 5 cm below the water surface in the jar[60]. Flow velocity data was measured in advance without addition of minerals and EPS but in otherwise the same artificial seawater at same flow depth in the identical jar). The time series of turbulent velocity fluctuations are transformed into Fourier space to obtain turbulent kinetic energy spectrum. Turbulence dissipation rate is then estimated to be $\varepsilon \approx 0.02$ m^2·s^{-3} via matching the Kolmogorov spectrum with Taylor frozen turbulence approximation[74,75]. The resulting turbulent shear rate is $G = \sqrt{\varepsilon/\nu} = 140$ s^{-1} with the fluid viscosity estimated to be $\nu = 10^{-6}$ m^2·s^{-1}.

Initial flocculation rate. To quantify the stickiness of each floc sample, the IFR has been estimated. A high-resolution digital microscopy system was used to observe detailed floc structures and to carry out statistical analysis on the floc numbers at different time during the floc generation for 120 min. Particularly in the initial 10 mins, floc samplings were conducted every 0.5 min from the stirring jar to the

microscopy analysis because of the quick flocculation occurrence at the beginning. By monitoring this temporal evolution of floc numbers, two phases could be detected clearly. The first one was the IFR, where the floc number decreased (decay) due to the quick aggregation dominant process at the beginning. The second phase was the equilibrium state, in which the floc number gradually remained constant reflecting stability between aggregation and breakage (see Fig. 1a). All the floc samples were directly transfered from the running experiment in real-time to the microscope using wide mouth (>5 mm) plastic pipettes to minimize floc disturbance. To prevent squeezing samples, coverslips on the microscope glass slides were avoid. Floc samples were observed with a 10 times zoom-in screen on a DELL laptop by the camera software provided by AmScope Inc.

Equilibrium floc size and settling velocity. To quantify the floc size and settling velocity statistics, a settling column experiment is carried out for each case after the flocs have reached the equilibrim state. The size and settling velocity of flocs after reaching the equilibrium state were observed using a low intrusive LabSFLOC-2 system (the 2nd version of Laboratory Spectral Flocculation Characteristics instrument)[65] of the entire floc population for each sample being assessed. A floc sample can be extracted from its original water environment and is immediately transferred to the column using a modified pipette with wide mouth as much as possible. The vedio camera, the center of which is positioned 0.075 m above the base of the column, views all particles in the center of the column as they settle from within a predeterminded sampling volume. All of the flocs viewed by the camera, for each sample. Are measured both for floc size and settling velocity. Clear, gray-scale, 2-Dimensional optical images of the individual flocs are recorded by the CCD camera suite. The LabsFLOC-2 system used here can measure floc sizes of 8 mm in diameter and settling velocities approaching 45 mm·s^{-1}, providing the flexibility to measure both pure mud and other cohesive mixture sediment floc dynamics[65]. By implementing a sequence of image-analysis algorithms, the fractal dimension and other properties of a floc population may be computed. The data obtained from this LabSFLOC-2 system is both qualitative and quantitative.

Floc images analysis. Temporal microscopy images (six images for each sample at a given time covering as many flocs as possible) have been collected during flocs generation in a magnetic stirrer jar from beginning ($t = 0$ min) to the end ($t = 2$ hrs) for each case shown in Table 1. The samplings intervals were set to be every 0.5 min for the initial 10 mins, followed by every 1 min between $t = 10$ and 20 mins, every 2 mins between $t = 20$~40 mins, every 5 mins between $t = 40$~60 mins and every 10 mins between $t = 60$~120 mins. Floc numbers are counted semi-manually with the aid of ImageJ software and Matlab tool at different instants. By normalizing the floc numbers counted at different instants by the initial floc number (collected at 0 min) of each sample, flocculation evolution time series were obtained for each cases (Fig. 1a, c). IFR is then calculated by estimating the slope of the tendency line of the first 3 min of each time series.

The detected and counted floc numbers amount to hundreds to thousands individual flocs in the six microscopy images taken at every instant of each case. For the validity and reliability of the floc number data, multiple analysis has been conducted by two different workers. The data points are generally similar with <10 % in standard deviation for all samples. The results shown in Fig. 1 have been averaged by all the valid parallel data.

Equilibrium floc properties calculation. The equilibrium floc properties including, floc numbers, size, shape, and settling velocity were measured and analyzed from a series of floc images captured by the LabSFLOC-2 system[65]. The recorded high-speed videos of floc settling in a column were analyzed with MATLAB software routines based on the HR Wallingford Ltd DigiFloc software[76] and Java Script to semi-automatically process the digital recording images track to obtain floc size and settling velocity spectra[68,77]. Using the measured floc diameter D, settling velocity W_s, and floc shape, the modified Stoke's Law[78] was applied to estimate individual floc effective density ρ_e as[79]

$$\rho_e = \frac{18 W_s \rho_w \nu}{gD^2} f(\mathrm{Re}) \tag{1}$$

where the ρ_w is the saltwater density, ν is the kinematic viscosity, and g is gravitational acceleration. The sphere-equivalent floc diameter D is calculated by

$$D = \left(D_{\mathrm{major}} \cdot D_{\mathrm{minor}}\right)^{\frac{1}{2}} \tag{2}$$

where D_{major} and D_{minor} are associated with the measured major and minor axes correspondingly. The Oseen[80] correction factor f is written as:

$$f(\mathrm{Re}) = \frac{1}{1 + 0.1875\mathrm{Re}} \tag{3}$$

which accounts for higher particle Reynolds number effect and the particle Reynolds number is defined here as:

$$\mathrm{Re} = \frac{\rho_e W_s D}{\rho_w \nu} \tag{4}$$

When Re is much smaller than unity, the modified Stokes' law reduces to the commonly used Stokes' law[81,82]. By assuming floc has a fractal structure, the fractal dimension of floc n_f can be calculated via the following relationship:[83]

$$\left(\frac{D}{d}\right)^{n_f - 3} = \frac{\rho_e}{\rho_s - \rho_w} \tag{5}$$

in which the primary particle diameter d is specified to be 4 μm.

All the analyzed individual flocs in a given case were classified in 12 floc size bands. The physical properties shown in Fig. 3 are the counted floc numbers of each size band, the averaged settling velocity, effective density, and fractal dimension for each floc size band.

Data availability

The datasets presented in this study can be found in online repositories. The names of the repository and accession number can be found below: https://data.gulfresearchinitiative.org (https://doi.org/10.7266/n7-0nav-gs95).

Received: 15 January 2022; Accepted: 12 April 2023;
Published online: 24 April 2023

References

1. Tolhurst, T. J., Gust, G. & Paterson, D. M. The influence of an extracellular polymeric substance (EPS) on cohesive sediment stability. *In:* Proceedings in marine science (eds Winterwerp, J. C. & Kranenburg C.), 409–425 (Elsevier, 2002).
2. Maggi, F. Biological flocculation of suspended particles in nutrient-rich aqueous ecosystems. *J. Hydrol.* **376**, 116–125 (2009).
3. Dyer, K. R. Sediment processes in estuaries: future research requirements. *J. Geophys. Res. Oceans* **94**, 14327–14339 (1989).
4. McAnally, W. H. & Mehta, A. J. Significance of aggregation of fine sediment particles in their deposition. *Estuar. Coast. Shelf Sci.* **54**, 643–653 (2002).
5. Laverman, A. M., Van Cappellen, P., van Rotterdam-Los, D., Pallud, C. & Abell, J. Potential rates and pathways of microbial nitrate reduction in coastal sediments. *FEMS Microbiol. Ecol.* **58**, 179–192 (2006).
6. Hu, Y., Xiao, Y., Liao, K., Leng, Y. & Lu, Q. Development of microalgal biofilm for wastewater remediation: from mechanism to practical application. *J. Chem. Technol. Biotechnol.* **96**, 2993–3008 (2021).
7. Boyd, P. W. & Trull, T. W. Understanding the export of biogenic particles in oceanic waters: is there consensus? *Prog. Oceanogr.* **72**, 276–312 (2007).
8. Pivokonsky, M. et al. Current knowledge in the field of algal organic matter adsorption onto activated carbon in drinking water treatment. *Sci. Total Environ.* **799**, 149455 (2021).
9. Simon, M., Grossart, H. P., Schweitzer, B. & Ploug, H. Microbial ecology of organic aggregates in aquatic ecosystems. *Aquat. Microb. Ecol.* **28**, 175–211 (2002).
10. Vercruysse, K., Grabowski, R. C. & Rickson, R. J. Suspended sediment transport dynamics in rivers: Multi-scale drivers of temporal variation. *Earth-Sci. Rev.* **166**, 38–52 (2017).
11. Giri, S., Arbab, N. N. & Lathrop, R. G. Assessing the potential impacts of climate and land use change on water fluxes and sediment transport in a loosely coupled system. *J. Hydrol.* **577**, 123955 (2019).
12. Mehta, A. J., Hayter, E. J., Parker, W. R., Krone, R. B. & Teeter, A. M. Cohesive sediment transport. I: process description. *J. Hydraul. Eng.* **115**, 1076–1093 (1989).
13. Baugh, J. V. & Manning, A. J. An assessment of a new settling velocity parameterisation for cohesive sediment transport modeling. *Cont. Shelf Res.* **27**, 1835–1855 (2007).
14. Riazi, A., Vila-Concejo, A., Salles, T. & Türker, U. Improved drag coefficient and settling velocity for carbonate sands. *Sci. Rep.* **10**, 1–9 (2020).
15. Fennessy, M. J., Dyer, K. R. & Huntley, D. A. INSSEV: An instrument to measure the size and settling velocity of flocs in situ. *Mar. Geol.* **117**, 107–117 (1994).
16. Mikkelsen, O. & Pejrup, M. The use of a LISST-100 laser particle sizer for in-situ estimates of floc size, density and settling velocity. *Geo-Mar. Lett.* **20**, 187–195 (2001).
17. Smith, S. J. & Friedrichs, C. T. Size and settling velocities of cohesive flocs and suspended sediment aggregates in a trailing suction hopper dredge plume. *Cont. Shelf Res.* **31**, S50–S63 (2011).
18. Fettweis, M. & Baeye, M. Seasonal variation in concentration, size, and settling velocity of muddy marine flocs in the benthic boundary layer. *J. Geophys. Res. Oceans* **120**, 5648–5667 (2015).

19. Tran, D. & Strom, K. Suspended clays and silts: Are they independent or dependent fractions when it comes to settling in a turbulent suspension? *Cont. Shelf Res.* **138**, 81–94 (2017).
20. Many, G. et al. Geometry, fractal dimension and settling velocity of flocs during flooding conditions in the Rhône ROFI. *Estuar. Coast. Shelf Sci.* **219**, 1–13 (2019).
21. Law, B. A., Hill, P. S., Maier, I., Milligan, T. G. & Page, F. Size, settling velocity and density of small suspended particles at an active salmon aquaculture site. *Aquacult. Environ. Interact.* **6**, 29–42 (2014).
22. Prandle, D., Lane, A. & Manning, A. J. Estuaries are not so unique. *Geophys. Res. Lett.* **32**, 23 (2005).
23. Hill, P. S., Milligan, T. G. & Geyer, W. R. Contrls on effective settling velocity of suspended sediment in the Eel River flood plume. *Cont. Shelf Res.* **20**, 2095–2111 (2000).
24. Smith, S. J. & Friedrichs, C. T. Image processing methods for in situ estimation of cohesive sediment floc size, settling velocity, and density. *Limnol. Oceanogr. Methods* **13**, 250–264 (2015).
25. Lamb, M. P. et al. Mud in rivers transported as flocculated and suspended bed material. *Nat. Geosci.* **13**, 566–570 (2020).
26. Passow, U. Transparent exopolymer particles (TEP) in aquatic environments. *Progr. Oceanog.* **55**, 287–33 (2002).
27. Ye, L., Manning, A. J., Holyoke, J., Penaloza-Giraldo, J. A. & Hsu, T. J. The role of biophysical stickiness on oil-mineral flocculation and settling in seawater. *Front. Mar. Sci.* **8**, 628827 (2021).
28. Flemming, H.-C. & Wingender, J. The biofilm matrix. *Nat. Rev. Microbiol.* **8**, 623–633 (2010).
29. More, T. T., Yadav, J. S. S., Yan, S., Tyagi, R. D. & Surampalli, R. Y. Extracellular polymeric substances of bacteria and their potential environmental applications. *J. Environ. Manage.* **144**, 1–25 (2014).
30. Engel, A. The role of transparent exopolymer particles (TEP) in the increase in apparent particle stickiness (alpha) during the decline of a diatom bloom. *J. Plankton Res.* **22**, 485–497 (2000).
31. Sobeck, D. C. & Higgins, M. J. Examination of three theories for mechanisms of cation induced bioflocculation. *Water Res.* **36**, 527–538 (2002).
32. Nasser, M. S. & James, A. E. The effect of polyacrylamide charge density and molecular weight on the flocculation and sedimentation behaviour of kaolinite suspensions. *Sep. Purif. Technol.* **52**, 241–252 (2006).
33. Bolto, B. & Gregory, J. Organic polyelectrolytes in water treatment. *Water Res.* **41**, 2301–2324 (2007).
34. Nakazawa, Y. et al. Differences in removal rates of virgin/decayed microplastics, viruses, activated carbon, and kaolin/montmorillonite clay particles by coagulation, flocculation, sedimentation, and rapid sand filtration during water treatment. *Water Res.* **203**, 117550 (2021).
35. Tan, X. L., Zhang, G. P., Hang, Y. I. N. & Furukawaf, Y. Characterization of particle size and settling velocity of cohesive sediments affected by a neutral exopolymer. *Int. J. Sediment Res.* **27**, 473–485 (2012).
36. Curtis, A. S. G. & Hocking, L. M. Collision efficiency of equal spherical particles in a shear flow. The influence of London-van der Waals forces. *Trans. Faraday Soc.* **66**, 1381–1390 (1970).
37. Dobias, B. *In:* Coagulation and flocculation: theory and applications (ed. Dobias B.), 700–720 (CRC Press, 1993).
38. Cheng, S. Y. et al. Landfill leachate wastewater treatment to facilitate resource recovery by a coagulation flocculation process via hydrogen bond. *Chemosphere* **262**, 127829 (2021).
39. Kim, S. & Palomino, A. M. Polyacrylamide-treated kaolin: a fabric study. *Appl. Clay Sci.* **45**, 270–279 (2009).
40. Derjaguin, B. v. & Landau, L. Theory of the stability of strongly charged lyophobic sols and of the adhesion of strongly charged particles in solutions of electrolytes. *Prog. Surf. Sci.* **43**, 30–59 (1993).
41. Olphen, H. V. Dispersion and flocculation. *Mineral. Soc. Monogr.* **6**, 203–224 (1987).
42. Verwey, E. J. & Overbeek, J. T. *In:* Theory of the Stability of Lyophilic Colloids (eds. Verwey, E. J. & Overbeek, J. T.) 200–218 (Elsevier, 1948).
43. Ho, Q. N., Fettweis, M., Spencer, K. L. & Lee, B. J. Flocculation with heterogeneous composition in water environments: a review. *Water Res.* **213**, 118147 (2022).
44. Harris, R. H. & Ralph, M. The role of polymers in microbial aggregation. *Annu. Rev. Microbiol.* **27**, 27–50 (1973).
45. Theng, B. K. G. Clay-polymer interactions: summary and perspectives. *Clays Clay Miner.* **30**, 1–10 (1982).
46. Zhang, P. et al. Extracellular protein analysis of activated sludge and their functions in wastewater treatment plant by shotgun proteomics. *Sci. Rep.* **5**, 12041 (2015).
47. Nouha, K., Hoang, N., Song, Y., Tyagi, R. & Surampalli, R. Characterization of extracellular polymeric substances (Eps) produced by cloacibacterium normanense isolated from wastewater sludge for sludge settling and dewatering. *J. Civil Environ. Eng.* **5**, 191 (2015).
48. Schmidt, J. & Ahring, B. K. Extracellular polymers in granular sludge from different upflow anaerobic sludge blanket (UASB) reactors. *Appl. Microbiol. Biotechnol.* **42**, 457–462 (1994).
49. Shen, C., Kosaric, N. & Blaszczyk, R. The effect of selected heavy metals (Ni, Co and Fe) on anaerobic granules and their extracellular polymeric substance (EPS). *Water Res.* **27**, 25–33 (1993).
50. Passow, U. Formation of rapidly-sinking, oil-associated marine snow. *Deep Sea Res. Part II* **129**, 232–240 (2016).
51. Burd, A. B. et al. The science behind marine-oil snow and MOSSFA: past, present, and future. *Prog. Oceanogr.* **187**, 102398 (2020).
52. Gregson, B. H. et al. Marine oil snow, a microbial perspective. *Front. Mar. Sci* **8**, 11 (2021).
53. Chenu, C. & Guerif, J. Mechanical strength of clay minerals as influenced by an adsorbed polysaccharide. *Soil Sci. Soc. Am. J.* **55**, 1076–1080 (1991).
54. Parsons, D. R. et al. The role of biophysical cohesion on subaqueous bed form size. *Geophys. Res. Lett.* **43**, 1566–1573 (2016).
55. Fettweis, M. & Lee, B. J. Spatial and seasonal variation of biomineral suspended particulate matter properties in high-turbid nearshore and low-turbid offshore zones. *Water* **9**, 694 (2017).
56. Jackson, G. A. & Lochmann, S. Modeling coagulation of algae in marine ecosystems. *In:* Environmental particles (ed. Jackson, G. A.), 387–414 (CRC Press, 2018).
57. Winterwerp, J. C. et al. Flocculation and settling velocity of fine sediment. *In:* Proceedings in Marine Science (ed. Winterwerp, J. C.), 25–40 (Elsevier, 2002).
58. Sheremet, A., Sahin, C. & Manning, A. J. Flocculation: a general aggregation-fragmentation framework. *Coastal Eng. Proc.* **35**, 27 (2017).
59. Nouha, K., Kumar, R. S., Balasubramanian, S. & Tyagi, R. D. Critical review of EPS production, synthesis and composition for sludge flocculation. *J. Environ. Sci.* **66**, 225–245 (2018).
60. Ye, L., Manning, A. J. & Hsu, T. J. Oil-mineral flocculation and settling velocity in saline water. *Water Res.* **173**, 115569 (2020).
61. Jayathilake, P. G. et al. Extracellular polymeric substance production and aggregated bacteria colonization influence the competition of microbes in biofilms. *Front. Microbiol.* **8**, 1865 (2017).
62. Soulsby, R. L., Manning, A. J., Spearman, J. & Whitehouse, R. J. S. Settling velocity and mass settling flux of flocculated estuarine sediments. *Mar. Geol.* **339**, 1–12 (2013).
63. Spencer, K. L. et al. Quantification of 3-dimensional structure and properties of flocculated natural suspended sediment. *Water Res.* **222**, 118835 (2022).
64. Maggi, F., Mietta, F. & Winterwerp, J. C. Effect of variable fractal dimension on the floc size distribution of suspended cohesive sediment. *J. Hydrol.* **343**, 43–55 (2007).
65. Manning, A. J., Friend, P. L., Prowse, N. & Amos, C. L. Estuarine mud flocculation properties determined using an annular mini-flume and the LabSFLOC system. *Cont. Shelf Res.* **27**, 1080–1095 (2007).
66. Manning, A. J., Baugh, J. V., Spearman, J. R. & Whitehouse, R. J. Flocculation settling characteristics of mud: sand mixtures. *Ocean Dyn.* **60**, 237–253 (2010).
67. Winterwerp, J. C., Manning, A. J., Martens, C., De Mulder, T. & Vanlede, J. A heuristic formula for turbulence-induced flocculation of cohesive sediment. *Estuar. Coast. Shelf Sci.* **68**, 195–207 (2006).
68. Manning, A. J., Langston, W. J. & Jonas, P. J. C. A review of sediment dynamics in the Severn Estuary: influence of flocculation. *Mar. Pollut. Bull.* **61**, 37–51 (2010).
69. Deng, Z., He, Q., Chassagne, C. & Wang, Z. B. Seasonal variation of floc population influenced by the presence of algae in the Changjiang (Yangtze River) Estuary. *Mar. Geol.* **440**, 106600 (2021).
70. Khelifa, A., Hill, P. S. & Lee, K. A. Comprehensive numerical approach to predict oil-mineral aggregate (OMA) formation following oil spills in aquatic environments. *In:* International Oil Spill Conference (ed. Khelifa, A.), 873–877 (American Petroleum Institute, 2005).
71. Passow, U. & Ziervogel, K. Marine snow sedimented oil released during the Deepwater Horizon spill. *Oceanography* **29**, 118–125 (2016).
72. Daly, K. L., Passow, U., Chanton, J. & Hollander, D. Assessing the impacts of oil associated marine snow formation and sedimentation during and after the deepwater horizon oil spill. *Anthropocene* **13**, 18–33 (2016).
73. Dukhovskoy, D. S. et al. Development of the CSOMIO coupled ocean-oil-sediment-biology model. *Front. Mar. Sci.* **8**, 194 (2021).
74. Voulgaris, G. & Trowbridge, J. H. Evaluation of the acoustic Doppler velocimeter (ADV) for turbulence measurements. *J. Atmos. Ocean. Technol.* **15**, 272–289 (1998).
75. Huang, C. J., Ma, H., Guo, J., Dai, D. & Qiao, F. Calculation of turbulent dissipation rate with acoustic Doppler velocimeter. *Limnol. Oceanog. Methods* **16**, 265–272 (2018).
76. Benson, T. & Manning, A. J. Digifloc: the development of semi-automatic software to determine the size and settling velocity of flocs. *In*: HR Wallingford Report DDY0427-Rt*001* (ed. Manning, A. J.), 1–45 (HR Wallingford, 2013).

77. Uncles, R. & Mitchell, S. *In:* Estuarine and coastal hydrography and sediment transport. (eds. Uncles, R. & Mitchell, S.), 300–362 (Cambridge Univ. Press, 2017).
78. Stokes, G. G. *In:* On the effect of the internal friction of fluids on the motion of pendulums (ed. Stokes, G.), 80–86 (Pitt Press, Cambridge, 1851).
79. Manning, A. & Schoellhamer, D. Factors controlling floc settling velocity along a longitudinal estuarine transect. *Mar. Geol.* **345**, 266–280 (2013).
80. Oseen, C. *In:* Neuere methoden und ergebnisse in der hydrodynamik, akad (ed. Oseen, C.), 300–317 (Akademische Verlagsgesellschaft, Leipzig, 1927).
81. Dyer, K. R. & Manning, A. J. Observation of the size, settling velocity and effective density of flocs, and their fractal dimensions. *J. Sea Res.* **41**, 87–95 (1999).
82. Kranenburg, C. The fractal structure of cohesive sediment aggregates. *Estuar. Coast. Shelf Sci.* **39**, 451–460 (1994).
83. Winterwerp, J. C. & van Kesteren, W. G. *In:* Introduction to the physics of cohesive sediment dynamics in the marine environment. (ed. Winterwerp, J. C.), 500–528 (Elsevier, 2004).

Acknowledgements

This research was made possible by the National Science Foundation (OCE-1924532) and in part by a grant from the Gulf of Mexico Research Initiative to support CSOMIO (Consortium for Simulation of Oil-Microbial Interactions in the Ocean) (Grant no. SA18−10). AM's contribution toward this research was also partly supported by the National Science Foundation grant OCE−1736668. LY's contribution was also partly supported by Southern Marine Science and Engineering Guangdong Laboratory (Zhuhai) (Grant No. 311020003) and the National Natural Science Foundation of China (Grant no. 42106160).

Author contributions

L.Y. conceived and designed the main conceptual ideas of this work, processed the laboratory experiments, performed the floc samplings, and data analysis, and wrote the main parts of the manuscript; J.A.P. contributed to the analysis of the results and the revision of the manuscript; A.J.M. contributed to the Labsfloc-2 analysis and revision of the manuscript; J.H. contributed to the experimental jar testings and calibration of the turbulence data; T.-J. H. supervised the study and contributed to the interpretation of results and the writing of the paper; T.-J.H., A.J.M., and L.Y. contributed to the funding resources.

Competing interests

The authors declare no competing interests.

Additional information

Supplementary information The online version contains supplementary material available at https://doi.org/10.1038/s43247-023-00801-w.

Correspondence and requests for materials should be addressed to L. Ye.

Peer review information *Communications Earth & Environment* thanks the anonymous reviewers for their contribution to the peer review of this work. Primary Handling Editors: Edmond Sanganyado, Joe Aslin, and Clare Davis. Peer reviewer reports are available.

Reprints and permission information is available at http://www.nature.com/reprints

Publisher's note Springer Nature remains neutral with regard to jurisdictional claims in published maps and institutional affiliations.